

# Theoretical Study of the Mechanism of the Abstraction Reactions of Heavy Cyclopropenes by Alcohol

Jun Hsiao, Chao-Ying Lan, and Ming-Der Su\*

Department of Applied Chemistry, National Chiayi University, Chiayi 60004, Taiwan

Received: January 31, 2008; Revised Manuscript Received: March 24, 2008

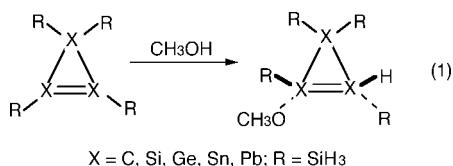
The potential energy surfaces for the abstraction reactions of heavy cyclopropenes with alcohol have been characterized in detail using density functional theory (B3LYP/LANL2DZdp), including zero-point corrections. Five heavy cyclopropene species including cyclopropene, cyclotrisilene, cyclotrigermene, cyclotritinene, and cyclotrileadene, have been chosen in this work as model reactants. All the interactions involve a hydrogen shift via a two-center transition state. The activation barriers and enthalpies of the reactions were compared in order to determine the relative reactivity of the heavy cyclopropenes. The present theoretical investigations suggest that the relative heavy cyclopropene reactivity increases in the order cyclopropene < cyclotrisilene < cyclotrigermene < cyclotritinene < cyclotrileadene. That is, for alcohol dehydrogenations there is a very clear trend toward lower activation barriers and less endothermic reactions on going from C to Pb. Besides this, our theoretical findings indicate that the final abstraction–addition products should adopt the anti geometry, rather than the syn geometry, from a thermodynamic viewpoint. Furthermore, a configuration mixing model based on the work of Pross and Shaik is used to rationalize the computational results. The results obtained allow a number of predictions to be made.

## I. Introduction

Recently, it was demonstrated that the heavy analogues of carbon in group 14 are also capable of forming unsaturated three-membered-ring systems.<sup>1</sup> Despite much greater difficulties in the preparation of these three-membered-ring molecules compared with their carbon analogue (cyclopropene), they are becoming increasingly available, constituting a new highly promising and quickly developing class of organometallic compounds: heavy cyclopropenes.

Kira and co-workers reported that the reactions of cyclotrisilene with various alcohols such as methanol, ethanol, *tert*-butyl alcohol, and phenols all produced the corresponding anti adduct regio- and stereospecifically.<sup>1a</sup> See Scheme 1.

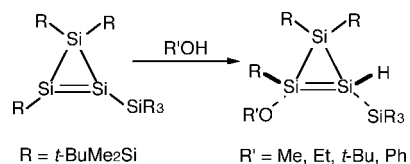
No quantum chemical calculations for such abstraction–addition reactions have yet been carried out, let alone a systematic theoretical study of geometric effects on the reactivities of heavy cyclopropene species. In order to elucidate the mechanism of the abstraction–addition reactions in these systems, we have undertaken an investigation of the potential energy surfaces of the following model reactions: by means of



density functional theory (DFT). At present, the specific heavy cyclopropene systems we have investigated are cyclopropene (1), cyclotrisilene (2), cyclotrigermene (3), cyclotritinene (4), and cyclotrileadene (5).

\* To whom correspondence should be addressed. E-mail: midesu@mail.ncyu.edu.tw.

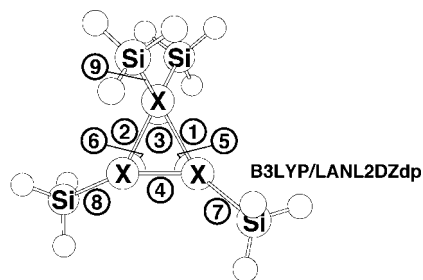
## SCHEME 1



The purpose of this work is fivefold: (i) to determine both the energies and structures of the transition states of the reactions; (ii) to obtain a detailed understanding of the energetics and kinetics of the transfer of a hydrogen atom from alcohol to the heavy cyclopropene; (iii) to probe geometric effects on the reactivities in a variety of heavy cyclopropenes; (iv) to understand the reason the final product adopts the anti geometry; (v) to obtain a better understanding of the origin of barrier heights for such abstraction–addition reactions.

## II. Theoretical Methods

All the geometries were fully optimized without imposing any symmetry constraints, although several optimized structures showed various elements of symmetry. For our DFT calculations, we used the hybrid gradient-corrected exchange functional proposed by Becke,<sup>2</sup> combined with the gradient-corrected correlation functional of Lee, Yang, and Parr.<sup>3</sup> Thus, the geometries of all the stationary points were fully optimized at the B3LYP level of theory. These B3LYP calculations were carried out with pseudorelativistic effective core potentials on group 14 elements modeled using the double- $\zeta$  (DZ) basis sets<sup>4</sup> augmented by a set of d-type polarization functions.<sup>5</sup> The DZ basis set for the hydrogen element was augmented by a set of p-type polarization functions (p exponents 0.356). The d exponents used for C, Si, Ge, Sn, and Pb were 0.587, 0.296, 0.246, 0.186, and 0.179, respectively. Accordingly, we denote our B3LYP calculations by B3LYP/LANL2DZdp. The spin-



Reactant (Singlet)

X	C	Si	Ge	Sn	Pb
①	1.563	2.313	2.496	2.872	3.109
②	1.563	2.313	2.518	2.908	3.127
③	49.79	54.35	55.71	55.84	56.76
④	1.316	2.113	2.304	2.707	2.868
⑤	65.10	62.82	63.11	62.75	62.94
⑥	65.10	62.82	62.16	61.39	62.29
⑦	1.849	2.315	2.405	2.618	2.708
⑧	1.850	2.315	2.411	2.627	2.721
⑨	1.885	2.336	2.409	2.601	2.679

**Figure 1.** B3LYP/LANL2DZdp-optimized geometries (in Å and deg) of the reactants **1–5** (singlet). For the relative energies for each species, see Table 1. Hydrogens are omitted for clarity.

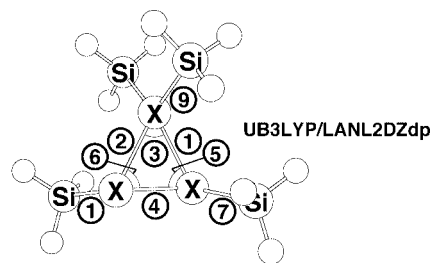
unrestricted (UB3LYP) formalism was used for the open-shell (triplet) species. The computed expectation values of the spin-squared operator ( $\langle S^2 \rangle$ ) were in the range of 2.001–2.012 for all the triplet species considered here, and they were therefore very close to the correct value of 2.0 for pure triplets, so that the geometries and energetics are reliable for this study. Frequency calculations were performed on all the structures to confirm that the reactants and products had no imaginary frequencies, and that the transition states (TSs) possessed only one imaginary frequency. The relative energies at 0 K were thus corrected for vibrational zero-point energies (ZPE, not scaled). All of the DFT calculations were performed using the Gaussian 03 package of programs.<sup>6</sup>

### III. Results and Discussion

#### 1. Geometries and Energetics of Heavy Cyclopropenes.

Before discussing the geometric optimizations and the potential energy surfaces for the chemical reactions studied in the present work, we shall first discuss the geometries and energies of the group 14 heavy cyclopropene reactants. The predicted geometric parameters for the closed-shell heavy cyclopropene species, based on the B3LYP/LANL2DZdp level of theory, are collected in Figure 1. The triplet structures of these heavy cyclopropenes (**1–5**) were also optimized (UB3LYP/LANL2DZdp), and their geometric parameters are shown in Figure 2. Their relative energies at the B3LYP level of theory are collected in Table 1. Their Cartesian coordinates calculated for the stationary points at the B3LYP level are available as Supporting Information. As mentioned earlier, we have used the SiH<sub>3</sub> substituent groups, instead of the *t*-BuMe<sub>2</sub>Si groups, in the heavy cyclopropene molecule for the sake of simplicity. Unfortunately, there are no experimental geometries yet available for the heavy cyclopropene species studied in the present work to allow a definitive comparison.<sup>7</sup>

By analogy with all other known dimetallenes (R<sub>2</sub>E=ER<sub>2</sub>; E = C, Si, Ge, Sn, and Pb),<sup>8</sup> it is inevitable that the two lowest energy states of the heavy cyclopropene analogues (**1–5**) are



Reactant (Triplet)

X	C	Si	Ge	Sn	Pb
①	1.485	2.354	2.595	2.946	3.087
②	1.485	2.355	2.592	2.918	3.181
③	57.40	58.45	59.07	61.51	62.17
④	1.494	2.299	2.478	2.999	3.237
⑤	59.79	60.77	61.41	58.77	60.33
⑥	59.79	60.77	61.51	59.70	57.49
⑦	1.832	2.336	2.440	2.651	2.745
⑧	1.832	2.336	2.441	2.653	2.714
⑨	1.901	2.331	2.408	2.599	2.667

**Figure 2.** B3LYP/LANL2DZdp-optimized geometries (in Å and deg) of the reactants **1–5** (triplet). For the relative energies for each species, see Table 1. Hydrogens are omitted for clarity.

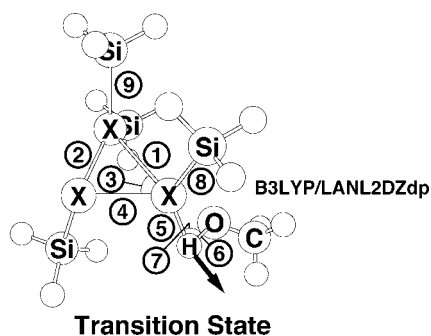
singlet and triplet.<sup>9</sup> These states are derived from the ground-state HOMO, an essentially bonding  $\pi$ -orbital based on the central doubly bonded X<sub>1</sub>=X<sub>2</sub> atoms, and the LUMO, an antibonding  $\pi$ -orbital on the X<sub>1</sub>=X<sub>2</sub> atoms. As one can see in Figures 1 and 2, those X<sub>1</sub>–X<sub>3</sub>, X<sub>2</sub>–X<sub>3</sub>, and X<sub>1</sub>=X<sub>2</sub> bond lengths for both singlet and triplet states show a monotonic increase down the group from carbon to lead. For instance, the X<sub>1</sub>=X<sub>2</sub> double bond distance increases in the order **1** (1.316 Å) < **2** (2.113 Å) < **3** (2.304 Å) < **4** (2.704 Å) < **5** (2.868 Å). Moreover, the singlet  $\angle X_1X_3X_2$  bond angles in cyclopropene (**1**), cyclotrisilene (**2**), cyclotrigermene (**3**), cyclotritinene (**4**), and cyclotrileadene (**5**), respectively, increase, as expected, in the given order: 49.8° < 54.4° < 54.7° < 55.8° < 56.8°. Likewise, the triplet  $\angle X_1X_3X_2$  bond angles follow the same trend: 57.4° (C) < 58.4° (Si) < 59.1° (Ge) < 61.5° (Sn) < 62.2° (Pb). Besides this, an interesting trend that can be observed in Figures 1 and 2 is the increase in the bond distances (i.e., X<sub>1</sub>=X<sub>2</sub>) and the increase in the bond angles (i.e.,  $\angle X_1X_3X_2$ ) on going from the singlet to the triplet state. Again, these can be easily understood using frontier orbital theory.<sup>9</sup>

Furthermore, the singlet–triplet energy separations ( $\Delta E_{st} = E_{\text{triplet}} - E_{\text{singlet}}$ ) of the group 14 heavy cyclopropenes is one of the crucial parameters in the present study. Our DFT calculations indicate that the singlet–triplet splittings for cyclopropene (**1**), cyclotrisilene (**2**), cyclotrigermene (**3**), cyclotritinene (**4**), and cyclotrileadene (**5**), are 47, 16, 5.6, 5.1, and –9.4 kcal/mol, respectively; i.e.,  $\Delta E_{st}$  decreases in the order **1** > **2** > **3** > **4** > **5**. That is, the magnitude of the energy difference between HOMO and LUMO for group 14 heavy cyclopropene systems becomes smaller as one proceeds along the series from C to Pb. In other words, our theoretical investigations demonstrate that the heavier the group 14 elements participating in the heavy cyclopropene system, the smaller its singlet–triplet energy splitting  $\Delta E_{st}$  is.<sup>10</sup> The reason for this is primarily because of the interaction of the high-lying  $\pi$ -orbitals of the endocyclic X<sub>1</sub>=X<sub>2</sub> double bonds in the framework and the low-lying  $\sigma^*$ -orbitals of the exocyclic X<sub>3</sub>–Si (X<sub>3</sub> = C, Si, Ge, Sn, and Pb)

**TABLE 1: Relative Energies for Singlet and Triplet Silylenes and for the Process Heavy Cyclopropene + CH<sub>3</sub>OH → Transition State → Abstraction Intermediate → Final Addition Products (anti and syn Geometries)<sup>a,b</sup>**

system	$\Delta E_{st}^c$ (kcal mol <sup>-1</sup> )	$\Delta E^\ddagger^d$ (kcal mol <sup>-1</sup> )	$\Delta H_{int}^e$ (kcal mol <sup>-1</sup> )	$\Delta H_{anti}^f$ (kcal mol <sup>-1</sup> )	$\Delta H_{syn}^g$ (kcal mol <sup>-1</sup> )
1 (cyclopropene)	+46.85	+51.94	+46.06	-20.03	-18.25
2 (cyclotrisilene)	+16.36	+42.49	+32.70	-51.71	-51.46
3 (cyclotrigermene)	+5.551	+34.48	+31.81	-36.26	-35.81
4 (cyclotritine)	+5.094	+32.69	+18.52	-21.29	-20.98
5 (cyclotrileadene)	-9.390	+26.83	+13.73	-16.56	-15.86

<sup>a</sup> At the B3LYP/LANL2DZdp levels of theory. For the B3LYP-optimized structures of the stationary points, see Figures 1, 2, 3, 4, 5, and 6. <sup>b</sup> Energy differences have been zero-point corrected. See the text. <sup>c</sup> Energy relative to the corresponding singlet state. A positive value means the singlet is the ground state. <sup>d</sup> The activation energy of the transition state, relative to the corresponding reactants. <sup>e</sup> The enthalpy of the intermediate, relative to the corresponding reactants. <sup>f</sup> The exothermicity of the anti product, relative to the corresponding reactants. <sup>g</sup> The exothermicity of the syn product, relative to the corresponding reactants.

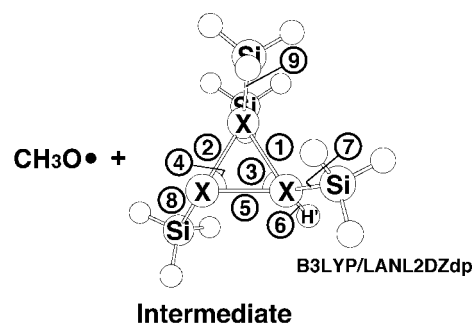


X	C	Si	Ge	Sn	Pb
①	1.644	2.584	2.956	3.177	3.468
②	1.490	2.261	2.436	2.811	2.892
③	58.86	54.71	51.75	53.40	51.26
④	1.341	2.306	2.568	3.075	3.193
⑤	1.209	1.548	1.628	1.799	1.992
⑥	1.462	1.550	1.494	1.495	1.626
⑦	123.70	99.09	91.77	86.19	86.43
⑧	1.987	2.346	2.445	2.628	2.694
⑨	1.894	2.358	2.435	2.609	2.659

**Figure 3.** Optimized geometries (in Å and deg) for the transition states (TS) of 1–5 (singlet) with CH<sub>3</sub>OH. All were calculated at the B3LYP/LANL2DZdp level of theory. For the relative energies for each species, see Table 1. The heavy arrow indicates the main component of the transition vector. Hydrogens are omitted for clarity.

bonds.<sup>11</sup> Additionally, it is well-known from a binding energy viewpoint that the  $\pi$ -bond strength of a double bond decreases from carbon to lead owing to the longer bond lengths when heavier group 14 elements are involved. As a result, combining all these important factors, the greater the atomic weight of the group 14 elements involved in the double bond of a heavy cyclopropene, the weaker its  $\pi$ -bond and the smaller the singlet–triplet energy gap  $\Delta E_{st}$  becomes. We shall use this conclusion to explain the origin of barrier heights for heavy cyclopropene abstraction–addition reactions in a later section.

**2. Transition States.** The optimized transition state structures (TS-C, TS-Si, TS-Ge, TS-Sn, and TS-Pb) together with an arrow indicating the main atom motions in the transition state eigenvector are shown in Figure 3. All five transition state structures show the same two-center pattern involving X (X = C, Si, Ge, Sn, and Pb) and hydrogen atoms. The transition state vectors represented by the heavy arrows in TS-C, TS-Si, TS-Ge, TS-Sn, and TS-Pb all are in accordance with the abstraction process, primarily the X–H bond stretching with a hydrogen (H') migrating to the X center. The B3LYP frequency calculations for the transition states TS-C, TS-Si, TS-Ge, TS-Sn, and

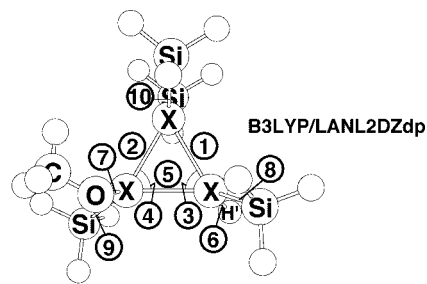


X	C	Si	Ge	Sn	Pb
①	1.574	2.356	2.576	3.028	3.273
②	1.484	2.318	2.531	2.902	3.106
③	57.99	59.58	59.54	63.19	64.55
④	64.12	61.21	61.29	58.78	58.99
⑤	1.482	2.309	2.521	2.878	3.021
⑥	1.100	1.486	1.552	1.733	1.786
⑦	1.882	2.320	2.410	2.594	2.667
⑧	1.832	2.328	2.458	2.656	2.733
⑨	1.887	2.326	2.417	2.599	2.657

**Figure 4.** Optimized geometries (in Å and deg) for the intermediates (Int) of 1–5 (singlet) with CH<sub>3</sub>OH. All were calculated at the B3LYP/LANL2DZdp level of theory. For the relative energies for each species, see Table 1. Hydrogens are omitted for clarity.

TS-Pb predict the unique imaginary frequency values of 721i, 1102i, 1278i, 1323i, and 1160i, respectively.

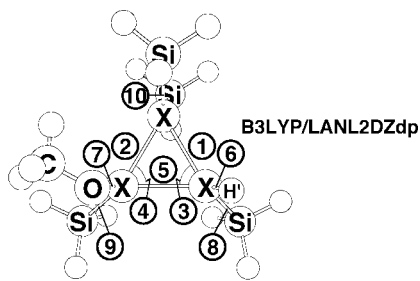
From Figure 3, one can easily see that increasing the atomic number of the attacked atom X in the heavy cyclopropene systems causes a large increase in the X–H' (H' = the abstracting hydrogen atom) distance. That is, the newly forming X–H' bond length increases in the order TS-C (1.21 Å) < TS-Si (1.55 Å) < TS-Ge (1.63 Å) < TS-Pb (1.79 Å) < TS-Sn (1.80 Å). Considering only the X–H' bond distance in formation, it is apparent that the TS-Sn and TS-Pb are closest to the intermediates (Int-Sn and Int-Pb, respectively), while TS-C and TS-Si are the most advanced transition state structures. According to the Hammond postulate,<sup>12</sup> the TS-C should have the highest and TS-Pb the smallest activation barrier. This was fully confirmed by our theoretical calculations. As already shown in Table 1, the barrier height (B3LYP) for the hydrogen-abstraction reaction decreases in the order TS-C (52 kcal/mol) > TS-Si (42 kcal/mol) > TS-Ge (34 kcal/mol) > TS-Sn (33 kcal/mol) > TS-Pb (27 kcal/mol). In other words, the greater the atomic number of the X center involved in the heavy cyclopropene skeleton, the smaller the hydrogen-abstraction barrier.



Product (anti)

X	C	Si	Ge	Sn	Pb
①	1.555	2.352	2.523	2.898	3.079
②	1.552	2.345	2.515	2.901	3.295
③	60.73	60.36	60.43	60.57	63.99
④	60.94	60.67	60.76	60.47	57.13
⑤	1.514	2.312	2.473	2.853	3.138
⑥	1.095	1.485	1.554	1.729	1.793
⑦	1.421	1.672	1.797	1.961	2.041
⑧	1.883	2.318	2.392	2.587	2.672
⑨	1.897	2.327	2.407	2.605	2.713
⑩	1.887	2.322	2.397	2.592	2.691

**Figure 5.** Optimized geometries (in Å and deg) for the products (anti) of 1–5 (singlet) with CH<sub>3</sub>OH. All were calculated at the B3LYP/LANL2DZdp level of theory. For the relative energies for each species, see Table 1. Hydrogens are omitted for clarity.



Product (syn)

X	C	Si	Ge	Sn	Pb
①	1.556	2.352	2.522	2.895	3.085
②	1.549	2.345	2.515	2.899	3.248
③	60.48	60.32	60.37	60.51	62.90
④	60.96	60.64	60.68	60.38	57.73
⑤	1.518	2.314	2.478	2.857	3.139
⑥	1.096	1.483	1.552	1.726	1.786
⑦	1.422	1.671	1.796	1.960	2.039
⑧	1.881	2.318	2.393	2.588	2.677
⑨	1.900	2.327	2.408	2.604	2.712
⑩	1.888	2.322	2.398	2.592	2.687

**Figure 6.** Optimized geometries (in Å and deg) for the products (syn) of 1–5 (singlet) with CH<sub>3</sub>OH. All were calculated at the B3LYP/LANL2DZdp level of theory. For the relative energies for each species, see Table 1. Hydrogens are omitted for clarity.

**3. Intermediates.** The structures of intermediates, i.e., the hydrogen-abstracting products (Int-C, Int-Si, Int-Ge, Int-Sn, and Int-Pb) optimized at the B3LYP level are shown in Figure 4, respectively. All the intermediates display similar X–H' bonding characteristics (X = C, Si, Ge, Sn, and Pb). As shown in Figure 4, our B3LYP calculations indicate that the X–H' distances in

the intermediates Int-C, Int-Si, Int-Ge, Int-Sn, and Int-Pb are 1.10, 1.49, 1.55, 1.73, and 1.79 Å, respectively.

Further, as discussed earlier, a heavy cyclopropene with more massive and less electronegative atoms in the double bond reaches the transition state relatively early, whereas a cyclopropene analogue with less massive but more electronegative atoms in the double bond arrives the transition state relatively late. The former is therefore predicted to undergo a less endothermic abstraction, which is borne out by our DFT calculations. For instance, our B3LYP calculations predict that their relative energies with respect to the corresponding reactants decrease in the order Int-C (46 kcal/mol) > Int-Si (33 kcal/mol) > Int-Ge (32 kcal/mol) > Int-Sn (19 kcal/mol) > Int-Pb (13 kcal/mol). Again, our theoretical model suggests that the greater the atomic number of the X center involved in the heavy cyclopropene skeleton, the smaller its hydrogen-abstraction enthalpy.

**4. Products.** The structures of the final abstraction–addition products with the anti geometry (Pro-A-C, Pro-A-Si, Pro-A-Ge, Pro-A-Sn, and Pro-A-Pb) generated at the B3LYP level of theory are illustrated in Figure 5. For comparison, the products with the syn geometry (Pro-S-C, Pro-S-Si, Pro-S-Ge, Pro-S-Sn, and Pro-S-Pb) at the same level of theory are given in Figure 6. Additionally, the calculated reaction enthalpies for such abstraction–addition products are collected in Table 1. As Figures 5 and 6 show, the order of X–OCH<sub>3</sub> bond lengths follows the same trend as the atomic weight of the atom X: Pro-A-C (1.42 Å) < Pro-A-Si (1.67 Å) < Pro-A-Ge (1.80 Å) < Pro-A-Sn (1.96 Å) < Pro-A-Pb (2.04 Å). The same effect can also be found in the final products with the syn geometry: Pro-S-C (1.42 Å) < Pro-S-Si (1.67 Å) < Pro-S-Ge (1.80 Å) < Pro-S-Sn (1.96 Å) < Pro-S-Pb (2.04 Å). These findings can be explained in terms of the expected atom size of the group 14 atom X, which increases as X changes from C to Pb.

Furthermore, one striking result that can be found in Table 1 is that the anti product is thermodynamically more stable than the corresponding syn product by about 1.8–0.31 kcal/mol. Thus, under these conditions, it is easy to see that the final addition product with the anti geometry should predominate in the product distributions. Our conclusion is consistent with the available experimental observations.<sup>1a</sup>

#### IV. Theoretical Model for the Reaction Barrier

In this section, an intriguing model for interpreting the reactivity of one hydrogen atom transfer reactions is provided by the so-called configuration mixing (CM) model, which is based on the work of Pross and Shaik.<sup>13,14</sup> According to the conclusions of this model, the energy barriers governing processes as well as the reaction enthalpies are proportional to the energy gap  $\Delta E_{st}$  ( $=E_{\text{triplet}} - E_{\text{singlet}}$ ) between the singlet and the triplet states of a heavy cyclopropene. In other words, the smaller the  $\Delta E_{st}$  of the heavy cyclopropene, the lower the barrier height, the larger the enthalpy, and, in turn, the faster the abstraction reaction.

Bearing the above conclusion in mind, we shall explain the origin of the observed trends as shown previously in the following discussion:

*Why is the alcohol dehydrogenation of heavier cyclopropene analogues more facile than that of lighter ones?*

The reason for this can be traced back to the singlet–triplet energy gap ( $\Delta E_{st}$ ) of the heavy cyclopropene analogue. As discussed in the present work, a heavier cyclopropene analogue possesses a smaller singlet–triplet splitting than a lighter one. Our model findings suggest that the singlet–triplet energy gap

( $\Delta E_{\text{st}}$ ) decreases in the order **1** (47 kcal/mol) > **2** (16 kcal/mol) > **3** (5.6 kcal/mol) > **4** (5.1 kcal/mol) > **5** (−9.4 kcal/mol). In other words, the magnitude of the singlet–triplet energy separation decreases with increasing atomic mass of the group 14 element. Furthermore, for the B3LYP/LANL2DZdp calculations on the aforementioned five systems, we obtain the following correlations (units in kcal/mol;  $r^2$  is the correlation coefficient):

$$\Delta E^\ddagger = 0.453\Delta E_{\text{st}} + 31.8 \quad (r^2 = 0.962) \quad (2)$$

$$\Delta H = 0.559\Delta E_{\text{st}} + 21.4 \quad (r^2 = 0.938) \quad (3)$$

As one can see in eqs 2 and 3, there exists a linear correlation between  $\Delta E_{\text{st}}$  and  $\Delta E^\ddagger$  (the abstraction barrier) as well as between  $\Delta H$  (the reaction enthalpy) and  $\Delta E^\ddagger$ . Consequently, our model calculations provide strong evidence that electronic factors resulting from the group 14 element should play a decisive role in determining the reactivity of a heavy cyclopropene.

## V. Conclusion

Taking all the aforementioned five reactions (heavy cyclobutene + CH<sub>3</sub>OH) studied in this paper together, one can draw the following conclusions:

(1) The abstraction–addition reactions of the heavy cyclopropenes proceed via a two-step abstraction–recombination path (formation of the two radicals and subsequent collapse to the final product).<sup>15</sup> Additionally, such abstraction reactions occur through a transition state characterized by the two atoms involved in the process.

(2) Heavy cyclopropenes undergo concerted dehydrogenation by reaction with an alcohol via a two-center transition state. As a result, the stereochemistry in the abstraction–addition product is preserved. This prediction correlates well with the available experimental findings.<sup>1a</sup>

(3) The reactivity of heavy cyclopropenes toward the alcohol increases with increasing atomic weight of the central atom X, i.e., in the order C < Si < Ge < Sn < Pb. More specifically, cyclotritinene and cyclotrilleadene can readily abstract a hydrogen atom from an alcohol, whereas cyclopropene is unreactive toward alcohols.

(4) Abstraction reactions with heavier cyclopropenes (such as cyclotritinene (**4**) and cyclotrilleadene (**5**)) are less endothermic than those with cyclopropene (**1**), reflecting the weaker Sn–H and Pb–H vs C–H bonds.

(5) Our theoretical findings strongly suggest that the final abstraction–addition product prefers to adopt the anti geometry, rather than the syn geometry, from a thermodynamic viewpoint. This conclusion is consistent with the available experimental works.<sup>1a</sup>

(6) If the heavier element congener of a three-membered-ring anti product is the primary product for heavy cyclopropene abstraction–addition reactions toward alcohol, then the singlet–triplet splitting of a heavy cyclopropene can be used as a diagnostic tool to predict the reactivities of various cyclopropene analogues.

(7) Electronic as well as steric factors should play a significant role in determining the chemical reactivity of heavy cyclopropene species, kinetically as well as thermodynamically.

We encourage experimentalists to carry out further experiments to confirm our predictions.

**Acknowledgment.** The authors are grateful to the National Center for High-Performance Computing of Taiwan for generous

amounts of computing time. They also thank the National Science Council of Taiwan for financial support. Special thanks are also due to referee 1 and referee 2 for very helpful suggestions and comments.

**Supporting Information Available:** Geometries and energetics. This material is available free of charge via the Internet at <http://pubs.acs.org>.

## References and Notes

- (1) For reviews about heavy cyclopropenes, see: (a) Kira, M. *J. Organomet. Chem.* **2004**, *689*, 4475. (b) Lee, V. Y.; Sekiguchi, A.; Ichinohe, M.; Fukaya, N. *J. Organomet. Chem.* **2000**, *611*, 228. (c) Sekiguchi, A.; Lee, V. Y. *Chem. Rev.* **2003**, *103*, 1429. (d) Lee, V. Y.; Ichinohe, M.; Sekiguchi, A. *J. Organomet. Chem.* **2003**, *685*, 168. (e) Lee, V. Y.; Sekiguchi, A. *Organometallics* **2004**, *23*, 2834.
- (2) (a) Becke, A. D. *Phys. Rev. A* **1988**, *38*, 3098. (b) Becke, A. D. *J. Chem. Phys.* **1993**, *98*, 5648.
- (3) Lee, C.; Yang, W.; Parr, R. G. *Phys. Rev. B* **1988**, *37*, 785.
- (4) (a) Dunning, T. H., Jr.; Hay, P. J. In *Modern Theoretical Chemistry*; Schaefer, H. F., III Ed.; Plenum: New York, 1976; pp 1–28. (b) Hay, P. J.; Wadt, W. R. *J. Chem. Phys.* **1985**, *82*, 270. (c) Hay, P. J.; Wadt, W. R. *J. Chem. Phys.* **1985**, *82*, 284. (d) Hay, P. J.; Wadt, W. R. *J. Chem. Phys.* **1985**, *82*, 299.
- (5) Check, C. E.; Faust, T. O.; Bailey, J. M.; Wright, B. J.; Gilbert, T. M.; Sunderlin, L. S. *J. Phys. Chem. A* **2001**, *105*, 8111.
- (6) Frisch, M. J.; Trucks, G. W.; Schlegel, H. B.; Scuseria, G. E.; Robb, M. A.; Cheeseman, J. R.; Zakrzewski, V. G.; Montgomery, J. A., Jr.; Vreven, T.; Kudin, K. N.; Burant, J. C.; Millam, J. M.; Iyengar, S. S.; Tomasi, J.; Barone, V.; Mennucci, B.; Cossi, M.; Scalmani, G.; Rega, N.; Petersson, G. A.; Nakatsuji, H.; Hada, M.; Ehara, M.; Toyota, K.; Fukuda, R.; Hasegawa, J.; Ishida, M.; Nakajima, T.; Honda, Y.; Kitao, O.; Nakai, H.; Klene, M.; Li, X.; Knox, J. E.; Hratchian, H. P.; Cross, J. B.; Adamo, C.; Jaramillo, J.; Gomperts, R.; Stratmann, R. E.; Yazyev, O.; Austin, A. J.; Cammi, R.; Pomelli, C.; Ochterski, J. W.; Ayala, P. Y.; Morokuma, K.; Voth, G. A.; Salvador, P.; Dannenberg, J. J.; Zakrzewski, V. G.; Dapprich, S.; Daniels, A. D.; Strain, M. C.; Farkas, O.; Malick, D. K.; Rabuck, A. D.; Raghavachari, K.; Foresman, J. B.; Ortiz, J. V.; Cui, Q.; Baboul, A. G.; Clifford, S.; Cioslowski, J.; Stefanov, B. B.; Liu, G.; Liashenko, A.; Piskorz, P.; Komaromi, I.; Martin, R. L.; Fox, D. J.; Keith, T.; Al-Laham, M. A.; Peng, C. Y.; Nanayakkara, A.; Challacombe, M.; Gill, P. M. W.; Johnson, B.; Chen, W.; Wong, M. W.; Gonzalez, C.; Pople, J. A. *Gaussian 03*; Gaussian, Inc.: Wallingford, CT, 2003.
- (7) However, some similar structures of cyclotrisilene and cyclotrigermene have been reported experimentally. See: (a) Ichinohe, M.; Matsuno, T.; Sekiguchi, A. *Angew. Chem., Int. Ed.* **1999**, *38*, 2194. (b) Iwamoto, T.; Kabuto, C.; Kira, M. *J. Am. Chem. Soc.* **1999**, *121*, 886. (c) Sekiguchi, A.; Yamazaki, H.; Kabuto, C.; Sakurai, H.; Nagase, S. *J. Am. Chem. Soc.* **1995**, *121*, 8025.
- (8) (a) Su, M.-D. *Inorg. Chem.* **2004**, *43*, 4846. (b) Su, M.-D. *J. Phys. Chem. A* **2004**, *108*, 823.
- (9) Jorgensen, W. L.; Salem, L. *The Organic Chemist's Book of Orbitals*; Academic Press: New York, 1973; pp 132–134.
- (10) Chen, C.-H.; Su, M.-D. *J. Phys. Chem. A*, in press.
- (11) This is well-known by the  $\pi$ – $\sigma^*$  conjugation concept. See: (a) Sekiguchi, A.; Lee, V. Y. *Chem. Rev.* **2003**, *103*, 1429. (b) Goller, A.; Heydt, H.; Clark, T. *J. Org. Chem.* **1996**, *61*, 5840. (c) Nyulaszi, L.; Schleyer, P. v. R. *J. Am. Chem. Soc.* **1999**, *121*, 6872. (d) Tsutsui, S.; Sakamoto, K.; Kabuto, C.; Kira, M. *Organometallics* **1998**, *17*, 3819. (e) Naruse, Y.; Ma, J.; Inagaki, S. *Tetrahedron Lett.* **2001**, *42*, 6553. (f) Su, M.-D. *Organometallics* **2004**, *23*, 2507.
- (12) Hammond, G. S. *J. Am. Chem. Soc.* **1954**, *77*, 334.
- (13) For details, see: (a) Shaik, S.; Schlegel, H. B.; Wolfe, S. In *Theoretical Aspects of Physical Organic Chemistry*; John Wiley & Sons Inc.: New York, 1992. (b) Pross, A. In *Theoretical and Physical Principles of Organic Reactivity*; John Wiley & Sons Inc.: New York, 1995. (c) Shaik, S. *Prog. Phys. Org. Chem.* **1985**, *15*, 197.
- (14) For the first paper that originated the CM model, see: (a) Shaik, S. *J. Am. Chem. Soc.* **1981**, *103*, 3692. (b) For about the most updated review of the CM model, see: Shaik, S.; Shurki, A. *Angew. Chem., Int. Ed.* **1999**, *38*, 586.
- (15) We have checked the possibilities of the existence of the other mechanisms (for instance, 1,2 addition, with or without catalysis by a second molecule of methanol). However, they always failed at the present computational method (B3LYP/LANL2DZdp).